A Platinum Open Access Journal for Organic Chemistry

Paper

Free to Authors and Readers | DOAJ Seal | Arkivoc **2026** (6) 202612612

Design, synthesis and metal ion sensing of novel indole-fluorene Schiff bases

Fangyuan Chen,[a,b] Chunyang Chen,[b] Guangcheng Lai,[b] Xiaolu Ouyang,[a]* and Hanfeng Cui[b]*

[a]Jiangxi Management Vocational College/Jiangxi Pharmaceutical Technician College, Nanchang 330200, China
[b]School of Pharmacy, Jiangxi University of Chinese Medicine, Nanchang 330004, China
Email: 183057728@qq.com cuihanfeng@126.com

Received 05-27-2026 **Accepted** 08-04-2026 **Published on line** 08-11-2026

Abstract

Schiff bases and their metal complexes have diverse applications in the fields of medicine, catalysis, analytical chemistry, corrosion inhibition and photochromism. A series of novel Schiff bases were synthesized via nitration, reduction and subsequent condensation with various substituted indole-3-carbaldehydes. The product structures were characterized by using FTIR, ^{1}H NMR, ^{13}C NMR and HRMS. Two representative molecules were shown to exhibit selective fluorescence enhancement toward Al^{3+}, Hg^{2+}, Fe^{3+} and Fe^{2+}, which can be ascribed to suppressed C=N isomerization and the chelation-enhanced fluorescence (CHEF) effect.

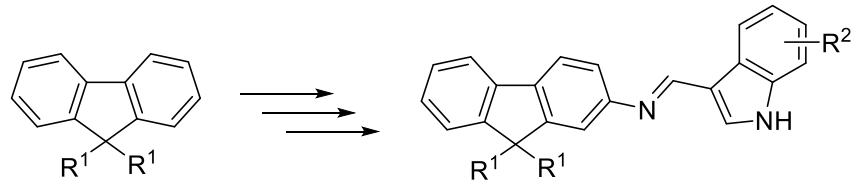

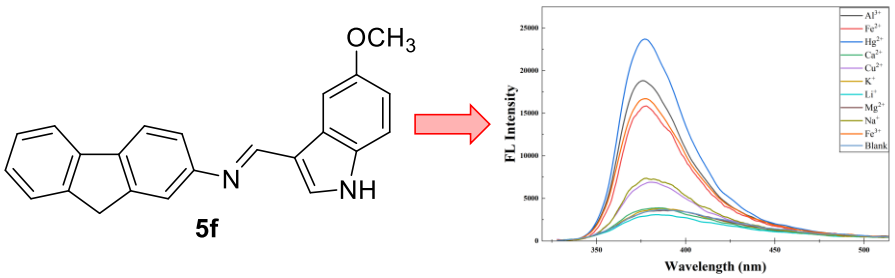

Keywords: Schiff bases, Fluorene, Indole-3-carbaldehyde, Metal ion sensing

Introduction

Schiff bases are an important class of organic compounds formed by the condensation of primary amines with active carbonyl compounds, characterized by the imine (–RC=N–) functional group. Since their discovery, Schiff bases have attracted sustained research interest in their structures and properties. Numerous studies have demonstrated that Schiff bases possess versatile application values covering analytical chemistry, biomedicine, catalysis, and corrosion inhibition.[1–3] Owing to their excellent coordination capability, Schiff bases have been extensively developed as chemical sensors in recent years for the detection of various analytes, emerging as one of the ideal sensing platforms for environmental and biological analysis. Through rational structural design of Schiff base molecules and coordination assembly with different metal ions, such probes can achieve sensitive detection of diverse targets, including metal cations (Hg^{2+}, Pb^{2+}, Cu^{2+}, Zn^{2+}, Ni^{2+}, Al^{3+}, Cr^{3+}, Fe^{3+}, etc.),[4–7] anions (CN^-, F^-, I^-, ClO^-, etc.),[8–11] pH variation,[12,13] as well as neutral analytes such as pesticides and insecticides in biological and environmental systems.[14–16] In 2025, Lin and co-workers[7] reported a ferrocenyl salicylaldehyde fluorene-based Schiff base fluorescent probe. Upon binding with metal ions, the probe exhibited obvious fluorescence enhancement. Mechanism investigations revealed that the turn-on fluorescence originated from the suppression of photoinduced electron transfer (PET) together with the chelation-enhanced fluorescence (CHEF) effect (Figure 1).[17–20] Accordingly, the design, synthesis, and application of novel Schiff bases and their complexes are of important research significance.

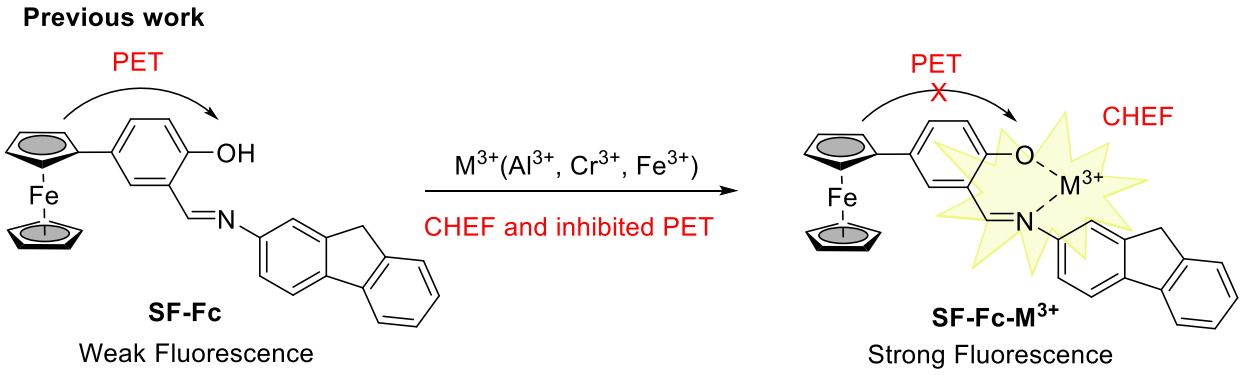

Figure 1. Fluorescent probe **SF-Fc** for recognition of trivalent metal ions.

Indole is an important nitrogen-containing aromatic heterocycle, which is widely distributed in natural products and synthetic functional molecules. Its derivatives have broad application prospects in agriculture, medicine, chemical sensing and other research fields.[21,22] Indole derivatives possess diverse biological activities and have been extensively developed in agricultural science as plant growth regulators,[23–25] pesticides,[26,27] antiviral agents[28–30] and fungicides.[31–33] For instance, indole-3-acetic acid is a classic phytohormone that regulates plant growth and development, thereby increasing crop yield. In the pharmaceutical field, indole-based compounds are widely exploited for anticancer,[34–37] antibacterial,[38–41] anti-inflammatory[42,43] and antiviral research.[44] As a representative drug, indomethacin, a non-steroidal anti-inflammatory agent, is clinically applied to treat acute and chronic rheumatoid arthritis, gouty arthritis, cancer pain, tenosynovitis and other inflammatory disorders. Apart from biological and medicinal values, indole derivatives also display outstanding potential in fluorescent chemical sensing. Cyanine dyes are typical functional fluorophores with indole skeletons. Benefiting from their long emission wavelength, good biocompatibility, high molar extinction coefficient and excellent tissue penetration, cyanine dyes show distinctive superiority in cellular and in vivo

bioimaging. Currently, cyanine-based fluorescent probes have been successfully used for trace detection of metal ions, anions, gas molecules, biological thiols, reactive oxygen species and other bioactive analytes.[45–47]

Fluorene skeleton features high molecular rigidity, excellent photoluminescence quantum yield and good structural modifiability, which can further improve the fluorescence stability and detection sensitivity of Schiff base probes.[48–50] In view of the excellent sensing performance of Schiff bases and indole derivatives, the fluorene skeleton with high rigidity was introduced into Schiff base molecules in this work. Two series of indole-fluorene Schiff base fluorescent probes were designed and synthesized (Figure 2), and their recognition and sensing performances toward metal ions were preliminarily investigated.

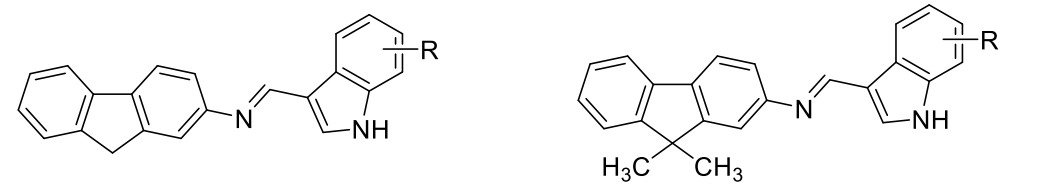

Figure 2. Two series of newly synthesized indole-fluorene Schiff bases.

Results and Discussion

Synthesis of indole-fluorene Schiff bases

The synthetic routes to two series of indole-fluorene Schiff bases (**5a**–**5h** and **9a**–**9f**) are illustrated in Scheme 1. For the synthesis of indole-di-H-fluorene Schiff bases **5a**–**5h**, fluorene **1** was used as the starting material and nitrated in acetic acid with concentrated nitric acid to introduce a nitro group at the 2-position, providing 2-nitrofluorene **2**.[51] Subsequently, reduction with zinc powder yielded 2-aminofluorene **3**.[51] Notably, zinc powder was pre-treated with dilute hydrochloric acid to remove the surface oxide layer prior to use. Finally, a series of indole-di-H-fluorene Schiff bases **5a**–**5h** were obtained via condensation reaction with substituted indole-3-carboxaldehydes **4** in the presence of glacial acetic acid as a catalyst.

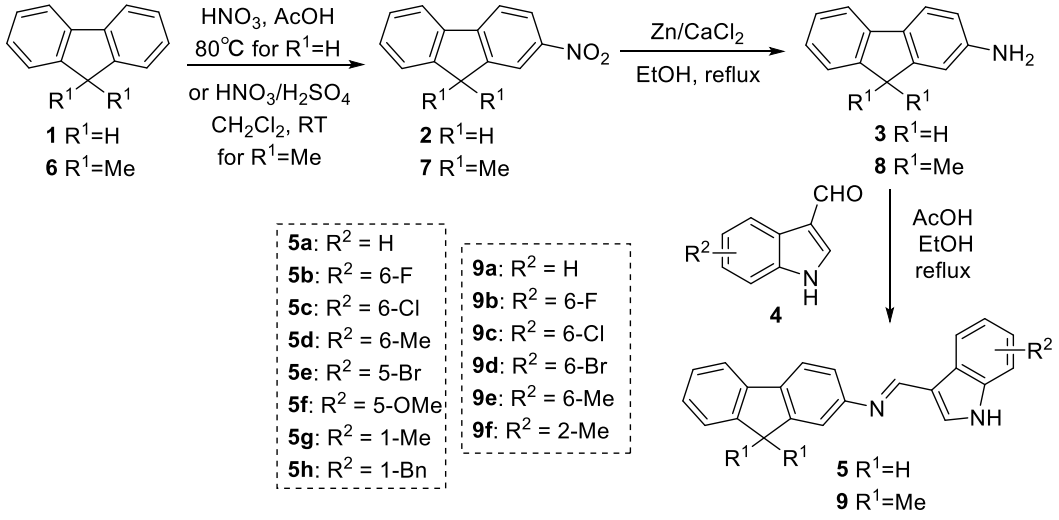

Scheme 1. Synthetic routes to the two series of Schiff bases **5** and **9**.

For the synthesis of indole-di-CH_3-fluorene Schiff bases **9a–9f**, 9,9-dimethylfluorene **6** served as the starting material. Unlike fluorene, the above-mentioned nitration conditions failed to afford satisfactory results for substrate **6**. Therefore, a concentrated HNO_3/H_2SO_4 mixture was employed as the nitrating reagent with dichloromethane as solvent at room temperature, affording 9,9-dimethyl-2-nitrofluorene **7** in good yield.[52] Following a similar reduction process and subsequent condensation with substituted indole-3-carboxaldehydes **4**,[53] a series of indole-di-CH_3-fluorene Schiff bases **9a–9f** were successfully synthesized.

Sensing properties of indole-fluorene Schiff bases for metal ions

Firstly, 5-bromo-substituted indole-di-H-fluorene Schiff base **5e** was chosen as a typical example to explore its recognition behavior toward diverse metal ions. In DMSO solution, the probe concentration was set to 1×10^{-4} M, and equivalent concentrations (1×10^{-4} M) of various metal ions, including Hg^{2+}, Al^{3+}, Fe^{3+}, Fe^{2+}, Cu^{2+}, Ca^{2+}, Mg^{2+}, Li^{+}, K^{+}, and Na^{+}, were added separately. Fluorescence measurements revealed that only Hg^{2+}, Al^{3+}, Fe^{3+} and Fe^{2+} induced distinct fluorescence enhancement of the probe, while negligible fluorescence change was observed for the other metal ions (Figure 3a). Such fluorescence enhancement may originate from the inhibition of C=N isomerization and the chelation-enhanced fluorescence (CHEF) effect induced by coordination between the probe and the four metal ions.

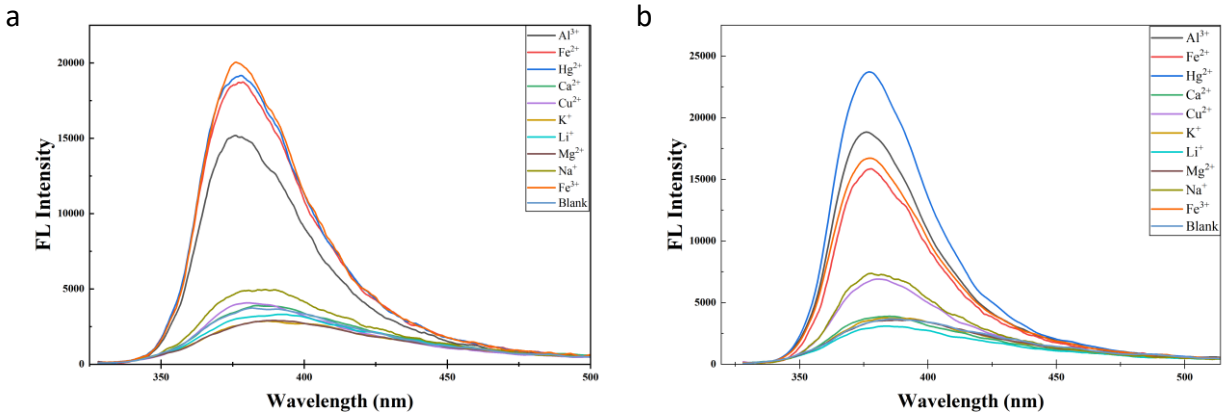

Figure 3. (a) Fluorescence spectra of **5e** with various metal ions (1 equiv.) in DMSO. (b) Fluorescence spectra of **5f** with various metal ions (1 equiv.) in DMSO.

In addition, 5-methoxy-substituted indole-di-H-fluorene Schiff base **5f**, which possesses electron-donating properties, exhibited similar recognition capability toward metal ions. Consistent with the above results, prominent fluorescence enhancement was observed upon addition of Hg^{2+}, Al^{3+}, Fe^{3+} and Fe^{2+}, while no distinct fluorescence response was seen for other metal ions (Figure 3b). By contrast, the 9,9-dimethylfluorene-based Schiff bases displayed inferior metal ion sensing capability. This performance difference can be ascribed to the steric hindrance originating from the gem-dimethyl groups, which distort the binding pocket and hinder effective metal coordination.

The unique selectivity toward Hg^{2+}, Al^{3+}, Fe^{3+} and Fe^{2+} can be rationalized by multiple factors. First, these four metal ions possess appropriate ionic radii and coordination geometries to form stable chelate complexes within the flexible binding cavity of the di-H-fluorene scaffold. Second, according to the Hard and Soft Acids and Bases (HSAB) principle, the imine nitrogen donors of the Schiff base skeleton exhibit favorable coordination compatibility with the target ions, which endows the probes with specific binding affinity toward these metal species. Photophysically, the coordination interaction effectively suppresses the photoinduced

electron transfer (PET) process and restricts the free rotation/isomerization of the C=N bond, together with the typical CHEF effect, collectively enabling the sensitive turn-on fluorescent response.

Subsequently, quantitative fluorescence titration of probe **5f** toward Fe^{2+} was implemented with Fe^{2+} equivalents ranging from 0 to 1.0 (Figure 4). The fluorescence intensity increased gradually and significantly with incremental addition of Fe^{2+} (0.1 eq, 0.25 eq, 0.5 eq, and 1.0 eq). To further clarify the recognition process, the *N*-methylated derivative **5g** was further investigated for comparison, and its fluorescence responses to Hg^{2+}, Al^{3+}, Fe^{3+} and Fe^{2+} were measured and found to be highly consistent with those of probes **5e** and **5f** (Figure S43).

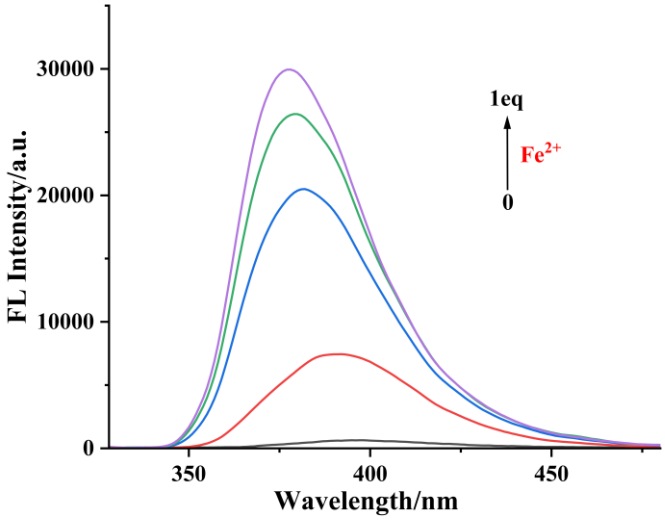

Figure 4. Fluorescent intensity of **5f** with the addition of Fe^{2+} in DMSO.

Based on the above results, we proposed two plausible scenarios for the recognition process: either the indole nitrogen atom is not involved in metal ion coordination during ion recognition, or the coordinated metal ions inhibit the isomerization of the Schiff base C=N bond together with other related sensing pathways. The present work only conducts preliminary fluorescence screening to validate the selective sensing performance of the probes. Further systematic investigations, including spectral characterization, binding behavior analysis, and theoretical simulation, will be performed to clarify the detailed sensing mechanism in our follow-up study.

Conclusions

In summary, two series of indole–fluorene Schiff bases were successfully synthesized and fully characterized. Their fluorescence sensing performances toward diverse metal cations were studied under uniform experimental conditions. These probes exhibited prominent fluorescence enhancement in the presence of Hg^{2+}, Al^{3+}, Fe^{3+}, and Fe^{2+}, revealing great potential as fluorescent sensors for the selective detection of these metal ions.

Experimental Section

General. All commercially available chemicals were used directly without further purification. Reactions were monitored by TLC using 0.25 mm GF254 silica gel plates, and flash column chromatography was performed with 200–300 mesh silica gel. FT-IR spectra were acquired on a Tianjin Gangdong FTIR-650 spectrometer. ^{1}H and ^{13}C NMR spectra were recorded on a Bruker Avance III HD 600 MHz NMR spectrometer, with chemical shifts referenced to TMS in ppm. ESI-HRMS was measured via a Thermo Scientific LTQ-Orbitrap mass spectrometer. Fluorescence spectra were recorded on FL970 spectrometers at 298 K.

Synthesis of 2-nitrofluorene (2). A 250 mL three-necked flask equipped with a thermometer and reflux condenser was charged with fluorene **1** (9.9 g, 60.0 mmol) and glacial acetic acid (90 mL). The mixture was stirred vigorously until the solid was completely dissolved. The solution was heated to 50 °C, and concentrated nitric acid (65 wt %, 14 mL) was added dropwise over 30 min. After the completion of the addition, the reaction temperature was elevated to 80 °C and held for 10 min. Upon cooling to room temperature, a yellow solid precipitate formed spontaneously. The resulting mixture was poured into 600 mL of ice water. The crude solid product was collected by vacuum filtration and washed with water (3 × 100 mL), then dried under vacuum. Recrystallization from ethanol (300 mL) afforded 2-nitrofluorene **2** as orange-yellow needle-like crystals (11.4 g, 90% yield). mp 155–156 °C, consistent with literature data.[51]

Synthesis of 2-aminofluorene (3). A solution of $CaCl_2$ (anhydrous, 1.0 g) in water (2.0 mL) and zinc powder (30.0 g) were added to a stirred mixture of 2-nitrofluorene **2** (3.0 g, 14.0 mmol) and ethanol (50 mL). The resulting mixture was heated at reflux for 2 h. The hot suspension was filtered immediately through a preheated Büchner funnel, and the residue was washed with hot ethanol (5.0 mL). The combined filtrate was slowly introduced into vigorously stirred ice water (300 mL), yielding a white flocculent precipitate. The solid was collected by vacuum filtration and dried under vacuum. Recrystallization from ethanol afforded 2-aminofluorene **3** as colorless needle crystals (1.82 g, 72%). mp 133–135 °C, consistent with literature data.[51]

Synthesis of 9,9-dimethyl-2-nitrofluorene (7). A 100 mL three-necked flask was charged with 9,9-dimethylfluorene **6** (5.8 g, 30.0 mmol) and dichloromethane (30 mL). The mixture was stirred until full dissolution. Mixed acid (9 mL, HNO_3 (65 wt %)/H_2SO_4 (98 wt %), 2:1 v/v) was added dropwise slowly while the internal temperature was kept between 5 and 10 °C over 15 min; the solution turned yellow gradually during the addition. The mixture was stirred at room temperature for 5 h. The reaction mixture was slowly poured into vigorously stirred ice-cold ethanol (200 mL) to form a yellow precipitate. The crude solid was collected by vacuum filtration, washed sequentially with water (3 × 20 mL) and cold ethanol (2 × 10 mL), then dried under vacuum. Recrystallization from ethanol provided 9,9-dimethyl-2-nitrofluorene **7** as yellow crystals (5.0 g, 70% yield). mp 98–99 °C, consistent with literature data.[52]

Synthesis of 2-amino-9,9-dimethylfluorene (8). 2-Amino-9,9-dimethylfluorene **8** was synthesized following the procedure described for 2-aminofluorene **3**. Starting from 9,9-dimethyl-2-nitrofluorene **7** (3.0 g, 12 mmol), target compound **8** was isolated as a solid (2.0 g, 77% yield). mp 162–163 °C, consistent with literature data.[53]

General procedure for the synthesis of indole-fluorene Schiff bases (**5a-5i, 9a-9f**).[54] 2-Aminofluorene **3** or 2-amino-9,9-dimethylfluorene **8** (1.0 mmol) was added to a solution of the corresponding indole-3-carbaldehyde **4** (1.0 mmol) in absolute ethanol (10 mL). Glacial acetic acid (3–5 drops) was introduced as catalyst. The mixture was heated at reflux for 5–6 h. After cooling to room temperature, a pale yellow solid precipitated out. The crude solid was collected by vacuum filtration, rinsed with ethanol (3 × 5 mL), and dried under reduced pressure to give the desired Schiff base product.

***N*-(9*H*-Fluoren-2-yl)-1-(1*H*-indol-3-yl)methylimine (5a).** Light yellow solid. Yield: 93%. mp 243–244 °C. IR (KBr, ν_{max}, cm^{-1}): 3249, 2961, 1622, 1593, 1573, 1530, 1443, 1426, 1364, 1244, 1124, 1096, 873, 809, 767, 735. ^{1}H NMR (600 MHz, $CDCl_3$): δ 8.79 (s, 1H, CH=N), 8.58 (dd, *J* 6.6, 1.8 Hz, 1H, ArH), 8.50 (brs, 1H, NH), 7.82 (d, *J* 8.4 Hz, 1H, ArH), 7.79 (d, *J* 7.8 Hz, 1H, ArH), 7.73 (s, 1H, ArH), 7.56 (d, *J* 7.2 Hz, 1H, ArH), 7.48–7.46 (m, 2H, ArH), 7.40 (t, *J* 7.2 Hz, 1H, ArH), 7.36–7.30 (m, 4H, ArH), 3.97 (s, 2H, CH_2). ^{13}C NMR (150 MHz, $CDCl_3$): δ 153.4, 152.4, 144.4, 143.3, 141.7, 138.8, 136.8, 129.9, 126.8, 126.2, 125.3, 124.9, 123.8, 122.4, 121.9, 120.3, 119.9, 119.6, 117.6, 116.9, 111.2, 36.9. ESI-HRMS: *m/z* calcd for $C_{22}H_{17}N_2$ $[M+H]^+$ 309.13862; found 309.13647.

***N*-(9*H*-Fluoren-2-yl)-1-(6-fluoro-1*H*-indol-3-yl)methylimine (5b).** Light yellow solid. Yield: 89%. mp 233–234 °C. IR (KBr, ν_{max}, cm^{-1}): 3020, 2893, 1621, 1590, 1536, 1445, 1424, 1404, 1365, 1334, 1231, 1147, 1116, 1094, 1085, 951, 843, 813, 767, 734. ^{1}H NMR (600 MHz, $CDCl_3$): δ 8.75 (s, 1H, CH=N), 8.47 (dd, *J* 8.4, 5.4 Hz, 1H, ArH), 8.47 (brs, 1H, NH), 7.82 (d, *J* 8.4 Hz, 1H, ArH), 7.79 (d, *J* 7.8 Hz, 1H, ArH), 7.67 (s, 1H, ArH), 7.56 (d, *J* 7.8 Hz, 1H, ArH), 7.47 (s, 1H, ArH), 7.40 (t, *J* 7.2 Hz, 1H, ArH), 7.32–7.29 (m, 2H, ArH), 7.14 (dd, *J* 9.0, 1.8 Hz, 1H, ArH), 7.09 (dt, *J* 9.6, 2.4Hz, 1H, ArH), 3.96 (s, 2H, CH_2). ^{13}C NMR (150 MHz, $CDCl_3$): δ 160.7 (d, $J_{C\text{-}F}$ 198.8 Hz), 153.5, 152.6, 144.4, 143.3, 141.6, 139.0, 136.8 (d, $J_{C\text{-}F}$ 10.0 Hz), 130.3, 126.8, 126.2, 124.9, 123.6 (d, $J_{C\text{-}F}$ 7.5 Hz), 121.7, 120.3, 119.9, 119.6, 117.6, 116.9, 110.5 (d, $J_{C\text{-}F}$ 20.0 Hz), 97.7 (d, $J_{C\text{-}F}$ 21.2 Hz), 37.4. ESI-HRMS: *m/z* calcd for $C_{22}H_{16}FN_2$ $[M+H]^+$ 327.12920; found 327.12726.

1-(6-Chloro-1*H*-indol-3-yl)-*N*-(9*H*-fluoren-2-yl)methylimine (5c). Yellow solid. Yield: 78%. mp 219–220 °C. IR (KBr, ν_{max}, cm^{-1}): 3069, 3033, 2893, 2835, 1620, 1595, 1562, 1525, 1448, 1426, 1368, 1325, 1273, 1247, 1127, 1110, 903, 852, 815, 765, 730. ^{1}H NMR (600 MHz, $CDCl_3$): δ 8.75 (s, 1H, CH=N), 8.52 (d, *J* 8.4 Hz, 1H, ArH), 8.49 (brs, 1H, NH), 7.81 (d, *J* 8.4 Hz, 1H, ArH), 7.79 (d, *J* 7.2 Hz, 1H, ArH), 7.69 (s, 1H, ArH), 7.56 (d, *J* 7.8 Hz, 1H, ArH), 7.47 (s, 1H, ArH), 7.46 (d, *J* 1.8 Hz, 1H, ArH), 7.40 (t, *J* 7.2 Hz, 1H, ArH), 7.32–7.29 (m, 3H, ArH), 3.96 (s, 2H, CH_2). ^{13}C NMR (150 MHz, $CDCl_3$): δ 153.4, 152.1, 144.4, 143.3, 141.6, 139.1, 137.2, 130.4, 129.6, 126.8, 126.3, 124.9, 123.8, 123.5, 122.6, 120.3, 119.9, 119.6, 117.6, 116.9, 111.2, 36.9. ESI-HRMS: *m/z* calcd for $C_{22}H_{16}ClN_2$ $[M+H]^+$ 343.09965; found 343.09799.

***N*-(9*H*-Fluoren-2-yl)-1-(6-methyl-1*H*-indol-3-yl)methylimine (5d).** Light yellow solid. Yield: 82%. mp 213–215 °C. IR (KBr, ν_{max}, cm^{-1}): 3249, 2961, 1613, 1594, 1568, 1529, 1444, 1422, 1367, 1241, 1125, 1067, 947, 906, 840, 813, 740. ^{1}H NMR (600 MHz, $CDCl_3$): δ 8.76 (s, 1H, CH=N), 8.43 (d, *J* 8.4 Hz, 1H, ArH), 8.39 (brs, 1H, NH), 7.81 (d, *J* 8.4 Hz, 1H, ArH), 7.79 (d, *J* 7.8 Hz, 1H, ArH), 7.64 (d, *J* 1.8 Hz, 1H, ArH), 7.56 (d, *J* 7.8 Hz, 1H, ArH), 7.47 (d, *J* 1.2 Hz, 1H, ArH), 7.40 (t, *J* 7.2 Hz, 1H, ArH), 7.32–7.30 (m, 2H, ArH), 7.25 (s, 1H, ArH), 7.16 (dd, *J* 7.8, 0.6 Hz, 1H, ArH), 3.96 (s, 2H, CH_2), 2.52 (s, 3H, CH_3). ^{13}C NMR (150 MHz, $CDCl_3$): δ 154.0, 152.5, 144.4, 143.3, 141.7, 138.7, 137.3, 133.7, 129.5, 126.8, 126.1, 124.9, 123.6, 123.1, 121.9, 120.3, 120.0, 119.5, 117.6, 116.8, 111.2, 36.9, 21.8. ESI-HRMS: *m/z* calcd for $C_{23}H_{19}N_2$ $[M+H]^+$ 323.15427; found 323.15216.

1-(5-Bromo-1*H*-indol-3-yl)-*N*-(9*H*-fluoren-2-yl)methylimine (5e). Light yellow solid. Yield: 90%. mp 186–187 °C. IR (KBr, ν_{max}, cm^{-1}): 3022, 2889, 1621, 1594, 1562, 1524, 1477, 1440, 1365, 1277, 1237, 1096, 1049, 882, 800, 765, 731. ^{1}H NMR (600 MHz, $CDCl_3$): δ 8.76 (d, *J* 1.8 Hz, 1H, ArH), 8.73 (s, 1H, CH=N), 8.65 (brs, 1H, NH), 7.82 (d, *J* 8.4 Hz, 1H, ArH), 7.79 (d, *J* 7.8 Hz, 1H, ArH), 7.68 (s, 1H, ArH), 7.57 (d, *J* 7.2 Hz, 1H, ArH), 7.48 (d, *J* 1.2 Hz, 1H, ArH), 7.43 (dd, *J* 8.4, 1.8 Hz, 1H, ArH), 7.40 (t, *J* 7.2 Hz, 1H, ArH), 7.38–7.29 (m, 3H, ArH), 3.96 (s, 2H, CH_2). ^{13}C NMR (150 MHz, $CDCl_3$): δ 153.3, 151.9, 144.4, 143.3, 141.6, 139.1, 135.5, 130.8, 126.9, 126.8, 126.7, 126.3, 125.1, 125.0, 120.3, 119.9, 119.6, 117.6, 116.4, 112.7, 37.0. ESI-HRMS: *m/z* calcd for $C_{22}H_{16}BrN_2$ $[M+H]^+$ 387.04914; found 387.04749.

***N*-(9*H*-Fluoren-2-yl)-1-(5-methoxy-1*H*-indol-3-yl)methylimine (5f).** Brown-yellow solid. Yield: 91%. mp 180–183 °C. IR (KBr, ν_{max}, cm^{-1}): 3022, 2896, 1620, 1596, 1567, 1530, 1488, 1465, 1440, 1292, 1266, 1214, 1183, 1108, 1071, 1021, 924, 860, 832, 803, 772, 741, 732. ^{1}H NMR (600 MHz, $CDCl_3$): δ 8.76 (s, 1H, CH=N), 8.49 (brs, 1H, NH), 8.10 (d, *J* 3.0 Hz, 1H, ArH), 7.81 (d, *J* 8.4 Hz, 1H, ArH), 7.79 (d, *J* 7.8 Hz, 1H, ArH), 7.66 (s, 1H, ArH), 7.57

(d, *J* 7.2 Hz, 1H, ArH), 7.48 (d, *J* 1.2 Hz, 1H, ArH), 7.40 (t, *J* 7.2 Hz, 1H, ArH), 7.34–7.29 (m, 3H, ArH), 6.99 (dd, *J* 8.4, 2.4 Hz, 1H, ArH), 3.97 (s, 2H, CH_2), 3.96 (s, 3H, CH_3). ^{13}C NMR (150 MHz, $CDCl_3$): δ 155.8, 154.1, 152.5, 144.4, 143.3, 141.7, 138.8, 131.7, 130.5, 126.8, 126.2, 125.9, 125.0, 120.3, 120.0, 119.5, 117.6, 116.6, 114.1, 112.0, 103.8, 55.9, 37.0. ESI-HRMS: *m/z* calcd for $C_{23}H_{19}N_2O$ $[M+H]^+$ 339.14919; found 339.14713.

***N*-(9*H*-Fluoren-2-yl)-1-(1-methyl-1*H*-indol-3-yl)methylimine (5g).** Light yellow solid. Yield: 83%. mp 199–202 °C. IR (KBr, ν_{max}, cm^{-1}): 3249, 2961, 1614, 1594, 1572, 1530, 1442, 1420, 1370, 1245, 1125, 1088, 947, 908, 876, 833, 806, 734. ^{1}H NMR (600 MHz, $CDCl_3$): δ 8.75 (s, 1H, CH=N), 8.53 (d, *J* 7.8 Hz, 1H, ArH), 7.81 (d, *J* 7.8 Hz, 1H, ArH), 7.79 (d, *J* 7.2 Hz, 1H, ArH), 7.58 (s, 1H, ArH), 7.56 (d, *J* 7.2 Hz, 1H, ArH), 7.47 (d, *J* 1.2 Hz, 1H, ArH), 7.41–7.29 (m, 6H, ArH), 3.96 (s, 2H, CH_2), 3.89 (s, 3H, CH_3). ^{13}C NMR (150 MHz, $CDCl_3$): δ 153.6, 152.6, 144.4, 143.3, 141.7, 138.7, 137.9, 134.2, 126.7, 126.1, 126.1, 124.9, 123.3, 122.3, 121.6, 120.3, 120.0, 119.5, 117.6, 115.2, 109.5, 36.9, 33.4. ESI-HRMS: *m/z* calcd for $C_{23}H_{19}N_2$ $[M+H]^+$ 323.15427; found 323.15210.

1-(1-Benzyl-1*H*-indol-3-yl)-*N*-(9*H*-fluoren-2-yl)methylimine (5h). Yellow solid. Yield: 85%. mp 178–180 °C. IR (KBr, ν_{max}, cm^{-1}): 3020, 2893, 1621, 1594, 1571, 1536, 1465, 1452, 1391, 1355, 1304, 1167, 1108, 1094, 1085, 951, 810, 773, 749, 738. ^{1}H NMR (600 MHz, $CDCl_3$): δ 8.76 (s, 1H, CH=N), 8.57–8.55 (m, 1H, ArH), 7.81 (d, *J* 7.8 Hz, 1H, ArH), 7.79 (d, *J* 7.8 Hz, 1H, ArH), 7.64 (s, 1H, ArH), 7.56 (d, *J* 7.8 Hz, 1H, ArH), 7.47 (s, 1H, ArH), 7.40 (t, *J* 7.2 Hz, 1H, ArH), 7.38–7.29 (m, 8H, ArH), 7.21 (dd, *J* 7.8, 1.2 Hz, 2H, ArH), 5.40 (s, 2H, CH_2), 3.96 (s, 2H, CH_2). ^{13}C NMR (150 MHz, $CDCl_3$): δ 153.6, 152.5, 144.4, 143.3, 141.7, 138.8, 137.5, 136.3, 133.5, 128.9, 128.1, 127.1, 126.8, 126.3, 126.1, 124.9, 123.5, 122.4, 121.8, 120.3, 120.0, 119.6, 117.6, 115.7, 110.1, 50.6, 37.0. ESI-HRMS: *m/z* calcd for $C_{29}H_{23}N_2$ $[M+H]^+$ 399.18557; found 399.18347.

***N*-(9,9-Dimethyl-9*H*-fluoren-2-yl)-1-(1*H*-indol-3-yl)methylimine (9a).** Light yellow solid. Yield: 85%. mp 237–239 °C. IR (KBr, ν_{max}, cm^{-1}): 3065, 2956, 2920, 2858, 1591, 1444, 1360, 1274, 1261, 1245, 1155, 1022, 964, 894. ^{1}H NMR (600 MHz, DMSO-d_6): δ 11.76 (brs, 1H, NH), 8.80 (s, 1H, CH=N), 8.41 (d, *J* 7.8 Hz, 1H, ArH), 8.02 (s, 1H, ArH), 7.81 (dd, *J* 8.4, 1.8Hz, 1H, ArH), 7.78 (d, *J* 7.2 Hz, 1H, ArH), 7.52 (d, *J* 7.2 Hz, 1H, ArH), 7.49 (d, *J* 8.4 Hz, 1H, ArH), 7.42 (s, 1H, ArH), 7.32 (t, *J* 7.2 Hz, 1H, ArH), 7.29–7.18 (m, 4H, ArH), 1.47 (s, 6H, CH_3, CH_3). ^{13}C NMR (150 MHz, DMSO-d_6): δ 155.4, 155.1, 153.8, 153.1, 138.9, 137.6, 135.7, 133.9, 127.5, 127.2, 125.2, 123.3, 123.2, 122.4, 121.4, 121.1, 120.4, 120.1, 115.8, 115.6, 112.5, 46.9, 27.4. ESI-HRMS: *m/z* calcd for $C_{24}H_{21}N_2$ $[M+H]^+$ 337.16992; found 337.16818.

***N*-(9,9-Dimethyl-9*H*-fluoren-2-yl)-1-(6-fluoro-1*H*-indol-3-yl)methylimine (9b).** Light yellow solid. Yield: 85%. mp 204–205 °C. IR (KBr, ν_{max}, cm^{-1}): 3249, 2961, 2858, 1615, 1589, 1534, 1440, 1371, 1336, 1289, 1148, 1118, 954, 877, 838, 810, 734. ^{1}H NMR (600 MHz, $CDCl_3$): δ 8.75 (s, 1H, CH=N), 8.56 (dd, *J* 9.0, 5.4 Hz, 1H, ArH), 8.51 (brs, 1H, NH), 7.76 (d, *J* 7.8 Hz, 1H, ArH), 7.74 (d, *J* 7.2 Hz, 1H, ArH), 7.67 (s, 1H, ArH), 7.46 (d, *J* 7.2 Hz, 1H, ArH), 7.38–7.35 (m, 2H, ArH), 7.32 (dt, *J* 7.8, 1.2 Hz, 1H, ArH), 7.25 (dd, *J* 7.8, 1.8Hz, 1H, ArH), 7.13 (dd, *J* 9.0, 1.8Hz, 1H, ArH), 7.32 (dt, *J* 9.0, 2.4 Hz, 1H, ArH), 1.55 (s, 6H, CH_3, CH_3). ^{13}C NMR (150 MHz, $CDCl_3$): δ 160.7 (d, $J_{C\text{-}F}$ 198.8 Hz), 154.9, 153.7, 153.6, 152.6, 139.1, 136.9 (d, $J_{C\text{-}F}$ 10.0 Hz), 136.5, 130.4 (d, $J_{C\text{-}F}$ 2.5 Hz), 126.9, 126.7, 123.6 (d, $J_{C\text{-}F}$ 7.5 Hz), 122.6, 121.7, 120.5, 119.7, 119.6, 116.9, 115.7, 110.5 (d, $J_{C\text{-}F}$ 20.0 Hz), 97.7 (d, $J_{C\text{-}F}$ 21.2 Hz), 46.9, 27.3. ESI-HRMS: *m/z* calcd for $C_{24}H_{20}FN_2$ $[M+H]^+$ 355.16050; found 355.15829.

1-(6-Chloro-1*H*-indol-3-yl)-*N*-(9,9-dimethyl-9*H*-fluoren-2-yl)methylimine (9c). Light yellow solid. Yield: 89%. mp 217–218 °C. IR (KBr, ν_{max}, cm^{-1}): 3186, 3161, 3108, 1627, 1600, 1574, 1466, 1459, 1421, 1392, 1167, 1077, 1050, 969, 899, 879, 844, 757, 745, 730. ^{1}H NMR (600 MHz, DMSO-d_6): δ 9.87 (s, 1H, CH=N), 8.27 (d, *J* 3.0 Hz, 1H, ArH), 8.04 (d, *J* 8.4 Hz, 1H, ArH), 7.58 (s, 1H, ArH), 7.51 (t, *J* 6.6 Hz, 1H, ArH), 7.43–7.40 (m, 1H, ArH), 7.36 (t, *J* 7.2 Hz, 1H, ArH), 7.24 (d, *J* 8.4 Hz, 1H, ArH), 7.21–7.18 (m, 1H, ArH), 7.12–7.09 (m, 1H, ArH), 6.68 (s, 1H, ArH), 6.54–6.52 (m, 1H, ArH), 1.31 (s, 6H, CH_3, CH_3). ^{13}C NMR (150 MHz, DMSO-d_6): δ 155.6, 152.8, 148.9, 140.1, 138.1, 128.8, 127.8, 127.5, 125.6, 123.3, 123.0, 122.7, 121.4, 118.8, 118.5, 113.7, 112.9, 112.8, 108.9, 46.9, 27.4. ESI-HRMS: *m/z* calcd for $C_{24}H_{20}ClN_2$ $[M+H]^+$ 371.13095; found 371.12906.

1-(6-Bromo-1*H*-indol-3-yl)-*N*-(9,9-dimethyl-9*H*-fluoren-2-yl)methylimine (9d). Light yellow solid. Yield: 84%. mp 207–208 °C. IR (KBr, ν_{max}, cm^{-1}): 3251, 2960, 1611, 1593, 1567, 1525, 1443, 1419, 1367, 1240, 1122, 1087, 885, 838, 810, 757, 738. ^{1}H NMR (600 MHz, $CDCl_3$): δ 8.75 (s, 1H, CH=N), 8.48 (d, *J*8.4 Hz, 1H, ArH), 7.76 (d, *J* 7.8 Hz, 1H, ArH), 7.73 (d, *J* 7.2 Hz, 1H, ArH), 7.67 (s, 1H, ArH), 7.61 (d, *J* 1.2 Hz, 1H, ArH), 7.46 (d, *J* 7.2 Hz, 1H, ArH), 7.43 (dd, *J* 8.4, 1.8 Hz, 1H, ArH), 7.38–7.35 (m, 2H, ArH), 7.32 (dt, *J* 7.2, 1.2 Hz, 1H, ArH), 7.25 (dd, *J* 7.8, 1.8Hz, 1H, ArH), 1.55 (s, 6H, CH_3, CH_3). ^{13}C NMR (150 MHz, $CDCl_3$): δ 154.9, 153.7, 153.4, 152.5, 139.1, 137.6, 136.6, 130.4, 126.9, 126.8, 125.2, 124.1, 123.8, 122.6, 120.6, 119.7, 119.6, 117.3, 116.9, 115.7, 114.2, 46.9, 27.3. ESI-HRMS: *m/z* calcd for $C_{24}H_{20}BrN_2$ $[M+H]^+$ 415.08044; found 415.07910.

***N*-(9,9-Dimethyl-9*H*-fluoren-2-yl)-1-(6-methyl-1*H*-indol-3-yl)methylimine (9e).** Light yellow solid. Yield: 82%. mp 180–182 °C. IR (KBr, ν_{max}, cm^{-1}): 3064, 2956, 2920, 2858, 1591, 1568, 1443, 1368, 1261, 1166, 1120, 995, 950, 886. ^{1}H NMR (600 MHz, DMSO-d_6): δ 11.62 (brs, 1H, NH), 8.76 (s, 1H, CH=N), 8.26 (d, *J* 7.8 Hz, 1H, ArH), 7.93 (s, 1H, ArH), 7.80 (d, *J* 7.8Hz, 1H, ArH), 7.77 (d, *J* 7.8 Hz, 1H, ArH), 7.52 (d, *J* 7.2 Hz, 1H, ArH), 7.41 (d, *J* 1.2 Hz, 1H, ArH), 7.32 (t, *J* 7.2 Hz, 1H, ArH), 7.27 (t, *J* 7.2 Hz, 2H, ArH), 7.19 (dd, *J* 7.8, 1.8Hz, 1H, ArH), 7.02 (d, *J* 8.4 Hz, 1H, ArH), 2.43 (s, 3H, CH_3), 1.47 (s, 6H, CH_3, CH_3). ^{13}C NMR (150 MHz, DMSO-d_6): δ 155.4, 155.1, 153.8, 153.2, 139.0, 138.1, 135.6, 133.5, 132.5, 127.5, 127.2, 123.1, 123.1, 123.0, 121.1, 120.4, 120.1, 115.8, 115.7, 112.3, 46.9, 27.4, 21.9. ESI-HRMS: *m/z* calcd for $C_{25}H_{23}N_2$ $[M+H]^+$ 351.18557; found 351.18353.

***N*-(9,9-Dimethyl-9*H*-fluoren-2-yl)-1-(2-methyl-1*H*-indol-3-yl)methylimine (9f).** Light yellow solid. Yield: 85%. mp 111–113 °C. IR (KBr, ν_{max}, cm^{-1}): 3044, 2967, 2918, 2859, 1621, 1591, 1537, 1381, 1216, 1160, 1125, 1010, 968, 837. ^{1}H NMR (600 MHz, DMSO-d_6): δ 8.82 (s, 1H, CH=N), 8.36 (d, *J* 7.2 Hz, 1H, ArH), 7.80 (d, *J* 7.8 Hz, 1H, ArH), 7.77 (d, *J* 7.8 Hz, 1H, ArH), 7.52 (d, *J* 7.2 Hz, 1H, ArH), 7.44 (s, 1H, ArH), 7.36 (d, *J* 7.2 Hz, 1H, ArH), 7.32 (t, *J* 7.2 Hz, 1H, ArH), 7.27 (t, *J* 7.2 Hz, 1H, ArH), 7.22 (d, *J* 8.4 Hz, 1H, ArH), 7.16–7.12 (m, 2H, ArH), 2.66 (s, 3H, CH_3), 1.48 (s, 6H, CH_3, CH_3). ^{13}C NMR (150 MHz, DMSO-d_6): δ 154.7, 153.5, 153.2, 143.6, 138.7, 135.8, 135.1, 127.1, 126.7, 126.1, 122.8, 122.1, 121.4, 121.2, 120.8, 120.1, 119.8, 115.6, 115.5, 110.9, 46.6, 27.1, 11.8. ESI-HRMS: *m/z* calcd for $C_{25}H_{23}N_2$ $[M+H]^+$ 351.18557; found 351.18347.

Fluorescence spectra

Stock solutions of probes **5e** and **5f** (1.0×10^{-4} M) were prepared in pure DMSO. Fluorescence sensing performance of **5e** and **5f** toward ten metal ions was investigated under identical experimental conditions. Briefly, probe stock solution (1.0×10^{-4} M, 10 µL) was diluted with pure DMSO (80 µL), followed by the addition of aqueous metal ion solutions at equal molar concentration. All metal ion stock solutions (Hg^{2+}, Al^{3+}, Fe^{3+}, Fe^{2+}, Cu^{2+}, Ca^{2+}, Mg^{2+}, Li^+, K^+, Na^+) were prepared from their respective chloride salts ($HgCl_2$, $AlCl_3$, $FeCl_3$, $FeCl_2$, $CuCl_2$, $CaCl_2$, $MgCl_2$, LiCl, KCl, NaCl) using ultrapure water.

Acknowledgements

The authors are grateful to the School of Pharmacy, Jiangxi University of Chinese Medicine, Nanchang, China, for providing laboratory facilities and essential experimental conditions. This work was financially supported by the College Students' Innovation and Entrepreneurship Training Program of Jiangxi University of Chinese Medicine (Grant No. X202410412180, S202510412092).

Supplementary Material

Supplemental material for this article is available online.

References

1. Xie, H. J.; Niu, C.; Chao, Z. Y.; Mamat, N.; Aisa, H. A. *Heterocycl. Commun.* **2020**, *26*, 176-184. https://doi.org/10.1515/hc-2020-0115
2. Middya, P.; Chakravarty, Y.; Maity, S.; Chattopadhyay, S. *J. Coord. Chem.* **2023**, *76*, 1777-1790. https://doi.org/10.1080/00958972.2023.2280514
3. Kumar, M.; Singh, A. K.; Singh, V. K.; Yadav, R. K.; Singh, A. P.; Singh, S. *Coord. Chem. Rev.* **2024**, *505*, 215663. https://doi.org/10.1016/j.ccr.2024.215663
4. Chaturvedi, I.; Vyas, S.; Mishra, R. *Dyes Pigm.* **2025**, *239*, 112748. https://doi.org/10.1016/j.dyepig.2025.112748
5. Ullah, Q.; Khan, S. A.; Arifuddin, M.; Mohsin, M.; Kausar, S.; Fatema, N.; Ahmer, M. F. *J. Fluoresc.* **2025**, *35*, 543-557. https://doi.org/10.1007/s10895-023-03514-7
6. Kumar, G. G. V.; Settu, M.; Jeyakumar, J. E.; S, H. K.; Raju, V. *J. Fluoresc.* **2026**, *36*, 2633-2642. https://doi.org/10.1007/s10895-026-04730-7
7. Li, Z. H.; Xu, Y. X.; Liu, W. Q.; Li, Y. B.; Lin, Y. *Luminescence* **2025**, 40, e70391. https://doi.org/10.1002/bio.70391
8. Nazir, F.; Musawar, S. S.; Khan, A. A.; Akram, B.; Ahmed, F. *Chin. J. Struct. Chem.* **2025**, *44*, 100751. https://doi.org/10.1016/j.cjsc.2025.100751
9. Lee, S. A.; You, G. R.; Choi, Y. W.; Jo, H. Y.; Kim, A. R.; Noh, I.; Kim, S. J.; Kim, Y.; Kim, C. *Dalton Trans*. **2014**, *43*, 6650-6659. https://doi.org/10.1039/c4dt00361f
10. Gupta, V. K.; Mergu, N.; Kumawat, L. K.; Singh, A. K. *Talanta* **2015**, *144*, 80-89. https://doi.org/10.1016/j.talanta.2015.05.053
11. Zhang, Q.; Zhou, X.; Zhang, Z.; Shen, L. Y.; Wang, Z. Y.; Xu, H.; Redshaw, C.; Zhang, Q. L. *J. Mol. Struct*. **2025**, *1343*, 142876. https://doi.org/10.1016/j.molstruc.2025.142876
12. Feng, Q.; Li, Y. Y.; Wang, L. L.; Li, C.; Wang, J. M.; Liu, Y. Y.; Li, K.; Hou, H. W. *Chem. Commun.* **2016**, *52*, 3123-3126. https://doi.org/10.1039/c5cc10423h
13. Song, P. S.; Chen, X. T.; Xiang, Y.; Huang, L.; Zhou, Z. J.; Wei, R. R.; Tong, A. J. *J. Mater. Chem.* **2011**, *21*, 13470-13475. https://doi.org/10.1039/c1jm12098k
14. Xie, Y.; Yan, L. Q.; Tang, Y. J.; Tang, M. H.; Wang, S. Y.; Bi, L.; Sun, W. Y.; Li, J. P. *J. Fluoresc.* **2019**, *29*, 399-406. https://doi.org/10.1007/s10895-019-02348-6
15. Wang, J. L.; Wang, H.; Yang, S. X.; Tian, H. Y.; Liu, Y. G.; Hao, Y. F.; Zhang, J.; Sun, B. G. *Anal. Sci.* **2018**, *34*, 329-333. https://doi.org/10.2116/analsci.34.329
16. Maity, D.; Manna, A. K.; Karthigeyan, D.; Kundu, T. K.; Pati, S. K.; Govindaraju, T. *Chem. Eur. J.* **2011**, *17*, 11152-11161. https://doi.org/10.1002/chem.201101906
17. Huston, M. E.; Haider, K. W.; Czarnik, A. W. *J. Am. Chem. Soc.* **1988**, *110*, 13, 4460-4462.

https://doi.org/10.1021/ja00221a083
18. Nootem, J.; Daengngern, R.; Sattayanon, C.; Wattanathana, W.; Wannapaiboon, S.; Rashatasakhon, P.; Chansaenpak, K. *J. Photochem. Photobiol. A* **2021**, *415*, 113318. https://doi.org/10.1016/j.jphotochem.2021.113318
19. Patil, M.; Bothra, S.; Sahoo, S. K.; Rather, H. A.; Vasita, R.; Bendre, R.; Kuwar, A. *Sens. Actuators, B* **2018**, *270*, 200-206. https://doi.org/10.1016/j.snb.2018.05.022
20. Alici, O.; Aydin, D. *J. Photochem. Photobiol. A* **2021**, *404*, 112876. https://doi.org/10.1016/j.jphotochem.2020.112876
21. Kochanowska-Karamyan, A. J.; Hamann, M. T. *Chem. Rev*. **2010**, *110*, 4489-4497. https://doi.org/10.1021/cr900211p
22. Heravi, M. M.; Zadsirjan, V. *RSC Adv*. **2020**, *10*, 44247-44311. https://doi.org/10.1039/d0ra09198g
23. Zhang, M.; Gao, C. X.; Xu L.; Niu, H.; Liu, Q.; Huang, Y. X.; Lv, G. S.; Yang, H. S.; Li, M. H. *Cells* **2022**, *11*, 3250. https://doi.org/10.3390/cells11203250
24. Sun, X.; Wang, N.; Li, P.; Jiang, Z. Y.; Liu, X. Y.; Wang, M. C.; Su, Z. Z.; Zhang, C. L.; Lin, F. C.; Liang, Y. *Plant Cell Environ.* **2020**, *43*, 358-373. https://doi.org/10.1111/pce.13667
25. Gomes, G. L. B.; Scortecci, K. C. *Plant Biol*. **2021**, *23*, 894-904. https://doi.org/10.1111/plb.13303
26. Liu, J. B.; Shi, Y. B.; Tian, Z. C.; Li, F. Y.; Hao, Z. S.; Wen, W.; Zhang, L.; Wang, Y. H.; Li, Y. X.; Fan, Z. J. *J. Agric. Food Chem.* **2022**, *70*, 5197-5206. https://doi.org/10.1021/acs.jafc.1c08297
27. Lee, J.-H.; Kim, Y.-G.; Kim, M.; Kim, E.; Choi, H.; Kim, Y.; Lee, J. *Environ. Microbiol*. **2017**, *19*, 1776-1790. https://doi.org/10.1111/1462-2920.13649
28. De Meester, C. *Mutat. Res*. **1995**, *339*, 139-153. https://doi.org/10.1016/0165-1110(95)90008-X
29. Callaway, J. C. *J. Psychoactive Drugs* **2005**, *37*, 151-155. https://doi.org/10.1080/02791072.2005.10399796
30. Song, H. J.; Liu, Y. X.; Liu, Y. X.; Wang, L. Z.; Wang, Q. M. *J. Agric. Food Chem.* **2014**, *62*, 1010-1018. https://doi.org/10.1021/jf404840x
31. Zhang, Z. J.; Zeng, Y.; Jiang, Z. Y.; Shu, B. S.; Sethuraman, V.; Zhong, G. H. *Pest Manag. Sci*. **2018**, *74*, 1736-1746. https://doi.org/10.1002/ps.4873
32. Buaban, K.; Phutdhawong, W.; Teachowisan, T.; Phutdhawong, W. S. *Molecules* **2021**, *26*, 207. https://doi.org/10.3390/molecules26010207
33. Zhang, Z. J.; Jiang, Z. Y.; Zhu, Q.; Zhong, G. H. *J. Agric. Food Chem*. **2018**, *66*, 9598-9607. https://doi.org/10.1021/acs.jafc.8b02124
34. Pelz, N. F.; Bian, Z. G.; Zhao, B.; Shaw, S.; Tarr, J. C.; Belmar, J.; Gergg, C.; Camper, D. V.; Goodwin, C. M.; Arnold, A. L.; Sensintaffar, J. L.; Friberg, A.; Rossanese, O. W.; Lee, T.; Olejniczak, E. T.; Fesik, S. W. *J. Med. Chem.* **2016**, *59*, 2054-2066. https://doi.org/10.1021/acs.jmedchem.5b01660
35. Nishiguchi, G. A.; Atallah, G.; Bellamacina, C.; Burger, M. T.; Ding, Y.; Feucht, P. H.; Garcia, P. D.; Han, W.; Klivansky, L.; Lindvall, M. *Bioorg. Med. Chem. Lett.* **2011**, *21*, 6366-6369.

https://doi.org/10.1016/j.bmcl.2011.08.105
36. Ke, S. Y.; Yang, Z. W.; Zhang, Z. G.; Liang, Y.; Wang, K. M.; Liu, M. L.; Shi, L. Q. *Bioorg. Med. Chem. Lett.* **2014**, *24*, 1907-1911. https://doi.org/10.1016/j.bmcl.2014.03.011
37. Li, X. Y.; Inks, E. S.; Li, X. G.; Hou, J. N.; Chou, C. J.; Zhang, J.; Jiang, Y. Q.; Zhang, Y. J.; Xu, W. F. *J. Med. Chem*. **2014**, *57*, 3324-3341. https://doi.org/10.1021/jm401877m
38. Priya, B.; Utreja, D.; Sharma, S.; Kaur, G.; Madhvi. *Curr. Org. Chem*. **2023**, *27*, 941-961. https://doi.org/10.2174/1385272827666230901140611
39. Chaiyosang, B.; Kanokmedhakul, K.; Yodsing, N.; Boonlue, S.; Yang, J. X.; Wang, Y. A.; Andersen, R. J.; Yahuafai, J.; Kanokmedhakul, S. *Nat. Prod. Res.* **2022**, *36*, 4973-4981. https://doi.org/10.1080/14786419.2021.1914613
40. Minvielle, M. J.; Eguren, K.; Melander, C. *Chem. Eur. J*. **2013**, *19*, 17595-17602. https://doi.org/10.1002/chem.201303510
41. Zelante, T.; Puccetti, M.; Giovagnoli, S.; Romani, L. *Curr. Opin. Immunol*. **2021**, *70*, 27-32. https://doi.org/10.1016/j.coi.2020.12.004
42. Zhou, L.; Gongpan, P. C.; Fan, Q. F.; Na, Z.; Huang, F. M.; Ji, K. L.; Song, Q. S. *Nat. Prod. Res*. **2022**, *36*, 5235-5240. https://doi.org/10.1080/14786419.2021.1928119
43. Bhati, S. K.; Kumar, A. *Eur. J. Med. Chem.* **2008**, *43*, 2323-2330. https://doi.org/10.1016/j.ejmech.2007.10.012
44. Bi, W.; Bi, Y.; Xue, P.; Zhang, Y. R.; Gao, X. A.; Wang, Z. B.; Li, M.; Baudy-Floc'h, M.; Ngerebara, N.; Gibson, K. M.; Bi, L. R. *J. Med. Chem.* **2010**, *53*, 6763-6767. https://doi.org/10.1021/jm100529e
45. Mishra, A; Behera, R. K.; Behera, P. K.; Mishra, B. K.; Behera, G. B. *Chem. Rev*. **2000**, *100*, 1973-2012. https://doi.org/10.1021/cr990402t
46. Sun, W.; Guo, S. G.; Hu, C.; Fan, J. L.; Peng, X. J. *Chem. Rev*. **2016**, *116*, 7768-7817. https://doi.org/10.1021/acs.chemrev.6b00001
47. Li, X. Z.; Yang, Y. L.; Zhang, R. H.; Huang, W. *Chem. Soc. Rev*. **2025**, *54*, 11184-11225. https://doi.org/10.1039/d5cs00063g
48. Grimsdale, A. C.; Chan, K. L.; Martin, R. E.; Jokisz, P. G.; Holmes, A. B. *Chem. Rev.* **2009**, *109*, 897-1091. https://doi.org/10.1021/cr000013v
49. Zhang, J. F.; Zhou, Y.; Yoon, J.; Kim, J. S. *Chem. Soc. Rev*. **2011**, *40*, 3416-3429. https://doi.org/10.1039/c1cs15028f
50. Zhao, R. C.; Wu, Y. S.; Zhang, Y. Q.; Ling, J. B.; Liu, X. X.; Xiang, J. Q.; Zeng, X. C.; Chen, T. F. *Sci. China Chem*. **2022**, *65*, 694-698. https://doi.org/10.1007/s11426-021-1197-4
51. Rahimi, H.; Hosseinzadeh, R.; Tajbakhsh, M. *J. Photoch. Photobio. A* **2021**, *407*, 113049. https://doi.org/10.1016/j.jphotochem.2020.113049
52. Parth; Kaur, N.; Korkor, C.; Mobin, S. M.; Chibale, K.; Singh, K. *ChemMedChem* **2022**, *17*, e202200414. https://doi.org/10.1002/cmdc.202200414
53. Zhang, H.; Fan, J. L.; Dong, H. J.; Zhang, S. Z.; Xu, W. Y.; Wang, J. Y.; Gao, P.; Peng, X. J. *J. Mater. Chem. B* **2013**, *1*, 5450-5455. https://doi.org/10.1039/c3tb20646g

54. Marufa, S. S.; Rahman, T.; Rahman, M. M.; Rahman, M. M.; Khan, S. J.; Jahan, R.; Nishino, H.; Alam, M. S.; Haque, M. A. *RSC Adv*. **2024**, *14*, 35198-35214. https://doi.org/10.1039/d4ra04197f